# Phosphorus-containing stereocontrolled polyhydroxyalkanoates by yttrium-mediated ring-opening copolymerization of $\beta$-lactones

Ali Dhaini, Rama M. Shakaroun, Jérôme Ollivier, Ali Alaaeddine, Sophie M. Guillaume, Jean-François Carpentier

▶ **To cite this version:**

Ali Dhaini, Rama M. Shakaroun, Jérôme Ollivier, Ali Alaaeddine, Sophie M. Guillaume, et al.. Phosphorus-containing stereocontrolled polyhydroxyalkanoates by yttrium-mediated ring-opening copolymerization of $\beta$-lactones. European Polymer Journal, 2024, European Polymer Journal, 209, pp.112919. 10.1016/j.eurpolymj.2024.112919 . hal-04506365

**HAL Id: hal-04506365**
**https://hal.science/hal-04506365v1**

Submitted on 24 May 2024

**HAL** is a multi-disciplinary open access archive for the deposit and dissemination of scientific research documents, whether they are published or not. The documents may come from teaching and research institutions in France or abroad, or from public or private research centers.

L'archive ouverte pluridisciplinaire **HAL**, est destinée au dépôt et à la diffusion de documents scientifiques de niveau recherche, publiés ou non, émanant des établissements d'enseignement et de recherche français ou étrangers, des laboratoires publics ou privés.

Distributed under a Creative Commons Attribution - NonCommercial 4.0 International License

European Polymer Journal 209 (2024) 112919

Contents lists available at ScienceDirect

European Polymer Journal

journal homepage: www.elsevier.com/locate/europolj

# Phosphorus-containing stereocontrolled polyhydroxyalkanoates by yttrium-mediated ring-opening copolymerization of β-lactones

Ali Dhaini [a,1], Rama M. Shakaroun [a,1], Jérôme Ollivier [a], Ali Alaaeddine [b], Sophie M Guillaume [a,*], Jean-François Carpentier [a,*]

[a] Univ. Rennes, CNRS, Institut Des Sciences Chimiques de Rennes, UMR 6226, F-35042 Rennes, France
[b] Univ. Libanaise, Campus Universitaire Rafic Hariri Hadath, Faculté Des Sciences, Laboratoire de Chimie Médicinale et Des Produits Naturels, Beirut, Lebanon

ARTICLE INFO

*Keywords:*
Poly(3-hydroxybutyrate) (PHB)
Copolymers
Phosphinate
Ring-opening copolymerization (ROCOP)
β-Lactone
Mass spectrometry
Polyhydroxyalkanoate (PHA)

ABSTRACT

Poly(3-hydroxybutyrate) (PHB) polymers functionalized with pendent diphenyl-phosphinate moieties were prepared by the simultaneous ring-opening copolymerization (ROCOP) of racemic or enantiopure β-butyrolactone (*rac*- or (*S*)-BPL$^{Me}$, respectively) with racemic-(4-oxooxetan-2-yl)methyl diphenylphosphinate (*rac*-BPL$^{OP}$). The reactions were mediated by yttrium catalysts which tunable ancillary structure enabled preparing copolymers containing syndio-enriched ($P_r$ up to 0.84; $P_r$ is the probability of racemic linkage), atactic ($P_r \sim 0.50$) and highly isotactic ($P_r < 0.06$) poly(BPL$^{Me}$) (P(BPL$^{Me}$), aka PHB for polyhydroxybutyrate) segments, starting from *rac*-BPL$^{Me}$ or (*S*)-BPL$^{Me}$, respectively, as assessed by detailed NMR analyses of the copolymer samples. The amount of BPL$^{OP}$ incorporated within the P[(BPL$^{Me}$)$_x$-*co*-(BPL$^{OP}$)$_y$] samples were in line with the initial comonomer loadings (1.8–8.1 mol% vs. 2–10 mol%). The ROCOP was rather well-controlled affording linear α-isopropoxy, ω-crotonyl telechelic and cyclic random copolymers with $M_{n,NMR}$ up to 15,000 g.mol$^{-1}$ and $Đ_M = 1.34–1.95$. Detailed MALDI and high-resolution ESI mass spectrometric analyses evidenced the formation of three major series of macromolecules, namely the cyclic one and two linear ones end-capped with an α-isopropoxy and either an ω-hydroxy or a ω-crotonate groups; for each of these series, the populations containing $y = 0$, 1 or 2 BPL$^{OP}$ repeating units were unambiguously distinguished. The thermal characteristics of the P[(BPL$^{Me}$)$_x$-*co*-(BPL$^{OP}$)$_y$] copolymers were investigated by DSC and TGA, revealing in comparison to those of the parent PHB homopolymers, tunable features as a function of their molar mass, tacticity and BPL$^{OP}$ content.

## 1. Introduction

Polyhydroxyalkanoates (PHAs) have received massive interest in the past decades as alternatives to regular polyolefin-type materials, in particular for packaging as well as for medicine applications [1,2,3,4,5]. Their biocompatibility and (bio)degradability are most attractive features [6,7,8]. Many PHAs can be obtained by fermentation of sugar-resources by microorganisms [9,10]. An even wider variety of PHAs can be prepared by synthetic chemistry, notably by ring-opening polymerization (ROP) [11,12,13,14,15,16,17,18] of 4-membered β-lactones or, as more recently demonstrated, of 8-membered diolides [19,20]. These ROP synthetic routes enable fine tuning of the molar mass and dispersity, tacticity, end-group fidelity, and sometimes topology (linear vs cyclic macromolecules). Discrete metal-based catalysts stabilized by multidentate ancillary ligands, in particular those based on rare-earths such as yttrium, have proven especially performant in such ROP reactions towards engineered PHAs [19,21,22]. These metal-based systems also effectively copolymerized β-lactones bearing variable functional groups [23], and random, blocky as well as alternating copolymers have been thus prepared from β-butyrolactone (aka 4-methyl-β-propiolactone, BPL$^{Me}$), higher 4-alkyl-β-propiolactones, 4-alkoxymethylene-β-propiolactones (BPL$^{OR}$s), and alkyl malolactonates [24,25].

On the other hand, the preparation of PHAs, and more generally of polyesters, bearing phosphorus functional moieties remains quite limited. Such polymers may be of interest for a variety of applications thanks to the specific properties brought by the phosphorous moieties. Early examples include phosphonylation of an unsaturated aliphatic polyester, initially prepared from dimethyl adipate and *cis*-2-butene-1,4-diol; radical addition of HP(O)(OMe)$_2$ [26] onto the C = C bonds of the

* Corresponding authors.
*E-mail addresses:* sophie.guillaume@univ-rennes.fr (S.M. Guillaume), jean-francois.carpentier@univ-rennes.fr (J.-F. Carpentier).
[1] These two authors contributed equally to this work.

https://doi.org/10.1016/j.eurpolymj.2024.112919
Received 19 January 2024; Received in revised form 5 March 2024; Accepted 8 March 2024
Available online 11 March 2024
0014-3057/© 2024 The Author(s). Published by Elsevier Ltd. This is an open access article under the CC BY-NC license (http://creativecommons.org/licenses/by-nc/4.0/).

polymer backbone succeeded in up to 30 mol%, conferring flame-retardancy/self-extinguishing as well as $Cu^{2+}$-adsorption properties to the phosphonate-modified materials [27]. Similar subsequent studies and conclusions on flame retardancy performance were drawn on copolyesters made from phosphinated diols induced in polycondensation with various aromatic carboxylic diacids [28,29,30,31]. PHAs bearing phosphate pendent groups were also prepared via post-polymerization metathesis of copolymers prepared by ROP of lactide with β-heptenolactone; the pendent alkene groups in the copolymers underwent cross-metathesis with allyl dimethyl phosphate using Hoveyda-Grubbs second-generation catalyst [32]. Recently, the post-polymerization modification by thermal addition of a phosphine (P($n$Bu)$_3$, $PMe_2Ph$) on the crotonate end-groups of a poly(3-hydroxybutyrate) (PHB) prepared by ROP of BPL$^{Me}$ with a guanidine organocatalyst (TBD) was reported to provide α-phosphonium end-functionalized PHBs displaying surfactant properties [33]. Yet, to our knowledge, there is no example of a direct preparation of a PHA bearing phosphorus functional moieties by (co)polymerization of an adequate P-functionalized (co)monomer [34].

Herein, we report on the ring-opening copolymerization (ROCOP) of a functional β-lactone, namely racemic (4-oxooxetan-2-yl)methyl diphenylphosphinate (*rac*-BPL$^{OP}$), with BPL$^{Me}$. The reactions were mediated with yttrium catalyst systems, starting from racemic or enantiopure BPL$^{Me}$, so as to access a set of novel microstructurally-controlled polymers with tunable properties (Scheme 1). The resulting phosphinate-modified PHAs could feature valuable properties along those abovementioned (fire-retardancy, metal cation adsorption…).

## 2. Experimental section

**Material and methods.** All manipulations involving organometallic catalysts were performed under an inert atmosphere (argon, < 5 ppm $O_2$ and $H_2O$) using standard Schlenk, vacuum line, and glovebox techniques. Toluene was freshly distillated from Na/benzophenone under argon and degassed thoroughly by freeze–thaw-vacuum cycles prior to use. Isopropyl alcohol was distilled over Mg turnings under argon atmosphere and kept over activated 3–4 Å molecular sieves. {ONNO$^{tBu2}$}$H_2$ and {ONNO$^{Me2}$}$H_2$ proligands and the Y(N(SiHMe$_2$)$_2$)$_3$(THF)$_2$ precursor, used to prepare in situ the amido yttrium complexes **1a-b**, respectively, were synthesized according to the reported procedures [35,36]. Enantiopure (*S*)-BPL$^{Me}$ (>98 % ee) was prepared following literature procedures, by carbonylation of enantiopure propylene oxide [37], itself prepared by hydrolytic kinetic resolution of racemic propylene oxide (Sigma-Aldrich) [38].

## 3. Instrumentation and measurements

$^1$H (500 and 400 MHz), $^{13}$C{$^1$H} (125 and 100 MHz) and $^{31}$P{$^1$H} (162 MHz) NMR spectra were recorded on Bruker Avance Ascend 400 spectrometers at 25 °C. $^1$H and $^{13}$C{$^1$H} NMR spectra were referenced internally relative to $SiMe_4$ ($\delta = 0$ ppm) using the residual solvent resonances. $^{31}$P{$^1$H} NMR spectra were referenced externally to $H_3PO_4$ ($\delta = 0$ ppm). Coupling constants are reported in Hz.

Number-average molar mass ($M_{n,SEC}$) and dispersity ($Đ_M = M_w/M_n$) values of the copolymers were determined by size-exclusion chromatography (SEC) in THF (homopolymers) or chloroform (copolymers) at 30 °C (flow rate = 0.8 mL.min$^{-1}$) on a Polymer Laboratories PL50 apparatus equipped with a UV detector at 254 nm and a set of two ResiPore PLgel 3 µm MIXED-D 300 × 7.5 mm columns. The concentration of the polymer samples was 5 mg.mL$^{-1}$. All elution curves were calibrated with polystyrene standards; $M_{n,SEC}$ values of the PHAs were uncorrected for the possible difference in hydrodynamic radius vs. that

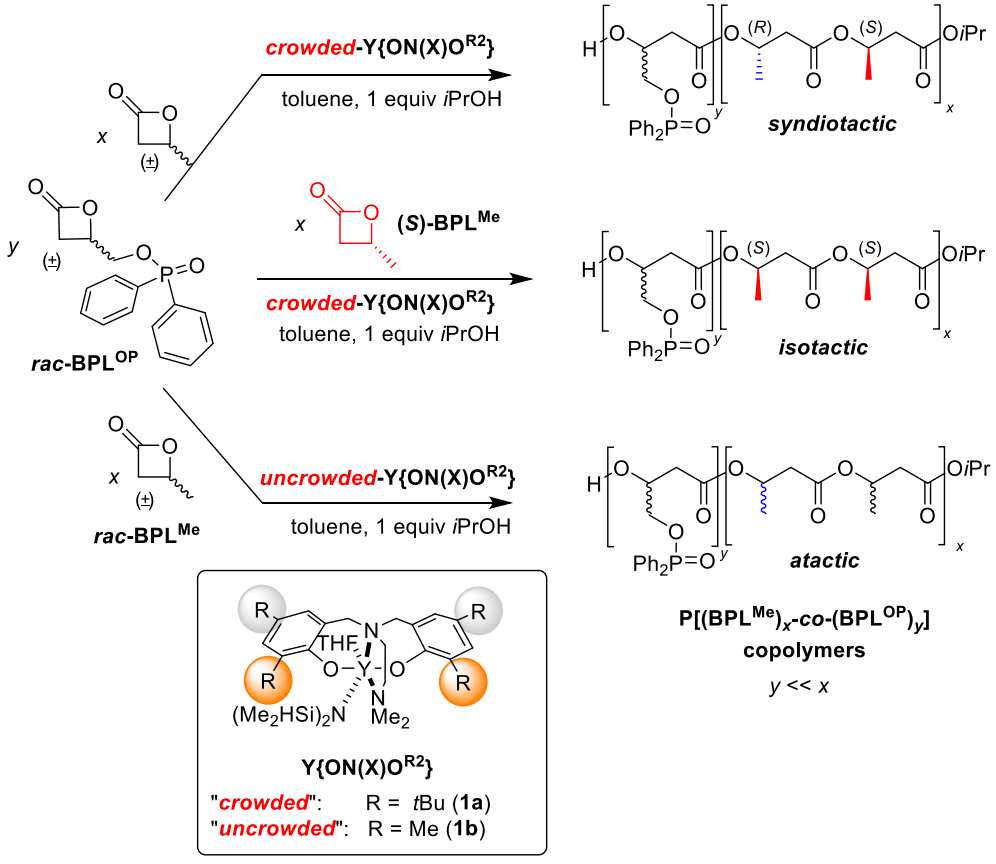


**Scheme 1.** Preparation of P[(BPL$^{Me}$)$_x$-*co*-(BPL$^{OP}$)$_y$] copolymers by one-pot, one-step simultaneous ring-opening copolymerization (ROCOP) of racemic or enantiopure β-butyrolactone (BPL$^{Me}$) with the racemic phosphinated β-lactone BPL$^{OP}$ using {Y{ON(N)O$^{R2}$} catalyst systems, with different stereoselectivity abilities.

of polystyrene.

The molar mass of PHA samples was also determined by $^1$H NMR analysis in $CDCl_3$ from the relative intensities of the signals of the PBPL$^{FG}$ repeating unit methine hydrogen ($\delta$ 4.99 ppm, –OC*H*($CH_2OCH(CH_3)$) and of the isopropyl chain-end (δ 1.19–1.25 ppm, ($CH_3$)$_2$CHO–); the accuracy of the $M_{n,NMR}$ values thus determined is evaluated to ± 200 g.mol$^{-1}$. Monomer conversions were calculated from $^1$H NMR spectra of the crude polymer samples in $CDCl_3$ by using the integration (Int.) ratios [Int.$_{PBPL(FG)}$ / (Int.$_{PBPL(FG)}$ + Int.$_{BPL(FG)}$)] of the methine hydrogens of PBPL$^{FG}$s (see above) and of the monomers ($\delta$ 4.66 ppm, BPL$^{Me}$; $\delta$ 4.78 ppm, BPL$^{OP(O)Ph2}$). The BPL$^{OP}$ content in the copolymers was determined by $^1$H NMR spectroscopy on reprecipitated polymers, considering the functional diphenylphosphino groups; the accuracy of the $^1$H NMR determination is evaluated to ± 0.5 %.

High resolution (error < 25 ppm) Matrix-Assisted Laser Desorption Ionization - Time of Flight (MALDI-ToF) mass spectra were performed using an ULTRAFLEX III TOF/TOF spectrometer (Bruker Daltonik Gmbh, Bremen, Germany) in positive ionization mode at the Centre Régional de Mesures Physiques de l'Ouest (CRMPO, ScanMAT UAR 2025, CNRS-Université de Rennes). Spectra were recorded using reflectron mode and an accelerating voltage of 25 kV. A mixture of a freshly prepared solution of the polymer in $CH_2Cl_2$ (HPLC grade, 10 mg.mL$^{-1}$) and the DCTB (*trans*-2-(3-(4-*tert*-butylphenyl)-2methyl-2-propenylidene)-malononitrile, and an acetonitrile solution of the cationizing agent ($CF_3CO_2Na$, 10 mg.mL$^{-1}$) were prepared. The solutions were combined in a ratio 1:1:1 *v/v/v* of matrix-to-sample-to-cationizing. The resulting solution (0.25–0.5 μL) was deposited onto the sample target (entry 4: MTP 384 ground steel, entry 5 Prespotted AnchorChip PAC II 384 / 96 HCCA) and air or vacuum dried.

High-resolution (error < 3 ppm) electrospray ionization (ESI) mass spectra were performed using an Orbitrap Q-Exactive (Thermo Fisher Scientific, Waltham (MA), USA) in positive ionization mode at CRMPO. The sample (Table 1, entry 5) was dissolved in methanol before being analyzed in solution by direct injection.

Description of the script used to process the mass spectrometric data, in order to establish the correspondence between the measured and the theoretical *m/z* values, based on the measurement precision, is provided in the Supporting Information.

Differential scanning calorimetry (DSC) analyses were performed on a DSC 2500 TA Instrument calibrated with indium using aluminum capsules (40 μL). The thermograms were recorded under a continuous flow of helium (25 mL min$^{-1}$) according to the following cycles: –80 to 200 °C at 10 °C min$^{-1}$; 200 to –80 °C at 10 °C min$^{-1}$; –80 °C for 5 min; –80 to 200 °C at 10 °C min$^{-1}$; 200 to –80 °C at 10 °C min$^{-1}$.

Thermal gravimetry analyses (TGA) were performed on a Metler Toledo TGA/DSC1 apparatus by heating the polymer samples at a rate of 10 °C min$^{-1}$ from 25 to 500 °C in a dynamic nitrogen atmosphere (flow rate = 50 mL min$^{-1}$).

**Synthesis of *racemic*-(oxiran-2-yl)methyl diphenylphosphinate (*rac*-G$^{OP}$).** In a Schlenk flask, under an inert argon atmosphere, *rac*-glycidol (2.00 g, 27.3 mmol) in THF (15 mL) was added to a solution of $ClP(O)Ph_2$ (7.73 g, 32.8 mmol) in THF (15 mL) at 0 °C. $NEt_3$ (3.32 g, 32.8 mmol) was then added dropwise to the reaction mixture at 0 °C. A white precipitate of $NEt_3HCl$ formed immediately. The reaction mixture was stirred overnight at room temperature, filtrated to remove $NEt_3HCl$ and the solution was concentrated in vacuum; the residue was purified by flash chromatography on silica gel (*n*-hexane/ethyl acetate 3:7 *v/v*) to give *rac*-G$^{OP}$ as a yellow viscous oil (5.25 g, 70 %). Spectroscopic data were consistent with those reported in the literature [39]. $^1$H NMR (400 MHz, $CDCl_3$, 25 °C) (Figure S1a): δ (ppm) $\delta$ 7.89–7.74 (m, 4H, Ph), 7.58–7.39 (m, 6H, Ph), 4.29 (ddd, $^2J_{H-H}$ = 11.4, $^3J_{H-H}$ = 7.6, $^3J_{H-P}$ = 3.2, 1H, POC*H*H), 3.93 (ddd, $^2J_{H-H}$ = 11.6, $^3J_{H-H}$ = 7.7, $^3J_{H-P}$ = 5.8, 1H, POCH*H*), 3.27 (ddt, $^3J_{H-H}$ = 5.8, 3.5, and 2.8, 1H, C*H*), 2.81 (dd, $^2J_{H-H}$ = 4.9, $^3J_{H-H}$ = 2.7, 1H, C*H*H epoxy), 2.64 (dd, $^2J_{H-H}$ = 4.9, $^3J_{H-H}$ = 2.7, 1H CH*H* epoxy). $^{31}$P{$^1$H} NMR (162 MHz, $CDCl_3$, 25 °C) (Figure S1b): δ (ppm) $\delta$ 32.82.

**Synthesis of *racemic*-(4-oxooxetan-2-yl)methyl diphenylphosphinate (*rac*-BPL$^{OP}$).** Following a literature procedure [40], under an inert argon atmosphere, a Schlenk flask was charged with [PPN]$^+$[Co(CO)$_4$]$^-$ (155 mg, 219 μmol). On a vacuum line, dry DME (15 mL) was syringed in the flask containing [PPN]$^+$[Co(CO)$_4$]$^-$ in order to solubilize it. The resulting solution was cannulated under argon into a degassed high-pressure stainless steel 100 mL-autoclave. A solution of *rac*-G$^{OP}$ (3.00 g, 10.95 mmol, 50 equiv vs. Co) in dry DME (15 mL) was added under argon in the autoclave, followed by dry $BF_3.Et_2O$ (30.9 mg, 219 μmol). The reactor was pressurized with carbon monoxide to 60 bars, and the reaction mixture was stirred with a magnetic bar for 2 days at 80 °C in an oil bath. Then, the reactor was cooled to room temperature, vented to atmospheric pressure, and the volatiles were removed under vacuum to give a green–blue viscous oil. The latter oil was solubilized in a minimum amount of ethyl acetate and then diluted with diethyl ether (150–200 mL) to return a precipitate (catalyst residues), which was filtered off. The remaining solution was dried under vacuum to give a yellow viscous oil, which was purified by flash column chromatography (*n*-hexane/ethyl acetate, gradient eluent of 2:8 to 1:9 *v/v*), providing *rac*-BPL$^{OP}$ as recovered as a white solid (3.30 g, 60 %) stored under argon. Crystals of *rac*-BPL$^{OP}$ suitable for X-ray diffraction analysis (Figure S7) were grown from a concentrated ethyl acetate solution at room temperature. $^1$H NMR (500 MHz, $CDCl_3$, 25 °C) (Figures S2a and S2b /COSY): $\delta$ (ppm) 7.88–7.77 (m, 4H, *o*-Ph), 7.59–7.52 (m, 2H, *p*-Ph), 7.52–7.42 (m, 4H, *m*-Ph), 4.76 (m, *J* = 4.2, 1H, *C*HOC(O)), 4.36 (ddd, $^2J_{H-H}$ = 12.2, $^3J_{H-H}$ = 6.5, $^3J_{H-P}$ = 2.9, 1H, C*H*HOP), 4.27 (ddd, $^2J_{H-H}$ = 12.2, $^3J_{H-H}$ = 6.8, $^3J_{H-P}$ = 4.0, 1H CH*H*OP), 3.58–3.49 (m, 2H, C$H_2$C(O)O). $^{13}$C{$^1$H} NMR (125 MHz, $CDCl_3$, 25 °C) (Figures S3 and S4/HMBC): $\delta$ (ppm) 166.9 (s, *C* = O), 132.8 and 132.7 (2 overlapping d, $^4J_{C-P}$ = 3.5, *p*-*C*H), 132.0 and 131.6 (2 d, $^2J_{C-P}$ = 12.8, *o*-*C*H), 130.7 and 130.3 (2 d, $^1J_{C-P}$ = 134.0 and 133.8, *ipso*-*C*H), 129.0 and 128.8 (2 d, $^3J_{C-P}$ = 2.2, *m*-*C*H), 68.6 (d, $^3J_{C-P}$ = 7.7, *C*HOC(O)), 63.5 (d, $^2J_{C-P}$ = 5.4 Hz, *C*$H_2$OP), 40.1 (s, *C*$H_2$C(O)O). $^{31}$P{$^1$H} NMR (162 MHz, $CDCl_3$, 25 °C): $\delta$ (ppm) 33.95 (Figure S5). ESI MS *m/z* obsvd = 303.0781 vs. *m/z* calcd for $C_{16}H_{16}O_4P$ [MH$^+$] = 303.0786 (Figure S6)

**Typical procedure for the ring-opening copolymerization of BPL$^{Me}$ with BPL$^{OP}$.** In a typical experiment, in the glovebox, a Schlenk flask was charged with Y(N(SiHMe$_2$)$_2$)$_3$(THF)$_2$ (20.8 mg, 35 μmol) and {ONNO$^{tBu2}$}H$_2$ (**1a**, 17.3 mg, 35 μmol), and toluene (0.5 mL) was next added. To this solution, *i*PrOH (191 μL of a 1 % (*v/v*) solution in toluene, 1 equiv vs. Y) was added under stirring at room temperature. After 5 min, a solution of *rac*-BPL$^{Me}$ (144 mg, 1.68 mmol, 48 equiv vs. Y) and *rac*-BPL$^{OP}$ (21.1 mg, 0.070 mmol, 2 equiv vs. Y) in toluene (0.9 mL) was added rapidly and the mixture was stirred at 20 °C for 3 h. The reaction was quenched by addition of acetic acid (ca. 0.5 mL of a 1.6 mol·L$^{-1}$ solution in toluene). The resulting mixture was concentrated to dryness under vacuum and the conversion was determined by $^1$H NMR analysis of the residue in $CDCl_3$. The crude polymer was then dissolved in $CH_2Cl_2$ (ca. 1 mL) and precipitated in cold pentane (ca. 5 mL), filtered and dried. Atactic P(BPL$^{Me}$-*co*-BPL$^{OP}$) samples were recovered as yellowish oils, while isotactic P((*iso*-BPL$^{Me}$)–*co*-BPL$^{OP}$) and syndio-enriched P((*syn*-BPL$^{Me}$)–*co*-BPL$^{OP}$) samples were recovered as colorless solids. $^1$H, $^{13}$C{$^1$H}, $^{31}$P{$^1$H}, COSY and HSQC NMR spectra are provided in the Supp. Info. as Figures S13–S43. $^1$H NMR (500 MHz, $CDCl_3$, 25 °C): $\delta$ (ppm) 7.88–7.77 (m, (4H)$_y$, *o*-Ph), 7.59–7.52 (m, (2H)$_y$, *p*-Ph), 7.52–7.42 (m, (4H)$_y$, *m*-Ph), 6.96 (m, 1H, $CH_3$-CH = C*H* crotonate), 5.77 (m, 1H, $CH_3$-C*H* = CH crotonate), 5.45 (m, (1H)$_y$, *C*HCH$_2$OP), 5.23 (m, (1H)$_x$, C*H* PHB segment), 5.01 (m, 1H, C*H* OiPr), 4.76 (m, *J* = 4.2, 1H, *C*HOC(O)), 4.2–4.1 (br m, (2H)$_y$, CHC$H_2$OP), 2.57–2.48 (m, (2H)$_{x+y}$, C*HH*C(O)O), 1.85 (d, 3H, C$H_3$-CH = CH crotonate), 1.28 (m, (3H)$_x$, C$H_3$ PHB segment + C$H_3$ OiPr). $^{13}$C{$^1$H} NMR (125 MHz, $CDCl_3$, 25 °C): δ (ppm) 169.4–169.2 (*C* = O), 144.5 ($CH_3$-CH = *C*H crotonate), 132.6, 131.8 and 128.9 (*C*H OPPh$_2$), 123.0 ($CH_3$-*C*H = CH crotonate), 68.1 (*C*HCH$_2$OP), 67.6 (*C*H PHB segment), 64.2 (*C*H$_2$OP), 43.3 (*C*H OiPr), 40.6 (*C*H$_2$ PHB segment), 34.3 (*C*H$_2$CHCH$_2$OP), 22.4 (s, *C*H$_3$-CH = CH crotonate), 20.0 (*C*H$_3$ PHB segment + *C*H$_3$ OiPr). $^{31}$P{$^1$H} NMR (162 MHz, $CDCl_3$, 25 °C):

$\delta$ (ppm) 32.8. MALDI-ToF and ESI mass spectra, see, Figures 3-5, Figs. S68-S71 and Table S2.

## 4. Results and discussion

The synthesis of *rac*-BPL$^{OP}$ monomer was performed by carbonylation of the corresponding epoxide, that is the diphenylphosphinate derivative of glycidol (*rac*-G$^{OP}$) (Scheme 2). Initial attempts using the ubiquitous [(Salph)Cr(THF)$_2$]$^+$[Co(CO)$_4$]$^-$ carbonylation catalyst [37,41,42,43,44,45] under a variety of reaction conditions returned in all cases the unreacted epoxide; this likely hinted at a deactivation of the catalyst by coordination of the phosphinate moiety (rather than the epoxide) onto the chromium center. In line with this hypothesis, effective carbonylation of *rac*-G$^{OP}$ was achieved using [PPN]$^+$[Co(CO)$_4$]$^-$/BF$_3$.Et$_2$O (PPN = bis(triphenylphosphine)iminium) [40]. *rac*-BPL$^{OP}$ was thus successfully obtained selectively in 60 % isolated yield and characterized by NMR and MS techniques and a single-crystal X-ray diffraction study (see the Supp. Info., Figures S2–S7, Table S1). Of note, the $^{13}$C NMR spectrum revealed the magnetic inequivalence of the two phenyl rings in the –OP(O)Ph$_2$ moiety due to the chiral center in the β-lactone ring (see Figure S3).

At first, the homopolymerization of *rac*-BPL$^{OP}$ was briefly investigated with yttrium complex **1a**, Y{ONNO$^{tBu2}$}/*i*PrOH, in toluene, considering the usually high activity and productivity of this catalyst system towards several other β-lactones (*vide supra*). Despite monomer loadings as low as 10–30 equiv vs. yttrium, the ROP proceeded very slowly and only incomplete conversions (<66 mol%) were reached after prolonged reaction times, at room temperature or even at 60 °C (Table 1).

A likely cause for the slow and incomplete propagation is the inhibition of the catalyst by the diphenylphosphinate functionality that may coordinate the yttrium center through its P=O group [46,47,48] and thereby prevent the effective coordination/activation of the β-lactone cycle. To further investigate this hypothesis, we studied the effect of a phosphinate additive on the ROP of a highly reactive β-lactone, namely *rac*-BPL$^{OAll}$ [25,49] (Scheme 3). In fact, while the ROP of 25 equiv of *rac*-BPL$^{OAll}$ mediated by **1a**/*i*PrOH (1:1) in toluene at room temperature proceeded with complete conversion within less than 1 h [25,49], the ROP of *rac*-BPL$^{OAll}$ under the same conditions but in the presence of 25 equiv of MePhP(O)OMe, only reached 19 % conversion after one day and 40 % after 3 days. This supported the competition of the C=O and P=O moieties of *rac*-BPL$^{OP}$ monomer to coordinate the metal center during the initiation/propagation steps of the ROP process.

The $^1$H and 2D COSY NMR spectra of the oligomers produced from the ROP of *rac*-BPL$^{OP}$ mediated by the **1a**/*i*PrOH system at room temperature and at 60 °C (Figures S8, S9, S11) show resonances consistent with linear chains bearing an α-isopropoxycarbonyl and an unsaturated ω-crotonyl-type end-groups, i.e. *i*PrO–[PBPL$^{OP}$]–C(O)CH=CHCH$_2$OP(O)Ph$_2$; yet, the presence of cyclic oligomers could not be assessed by this spectroscopic technique and hence, it cannot be excluded. The

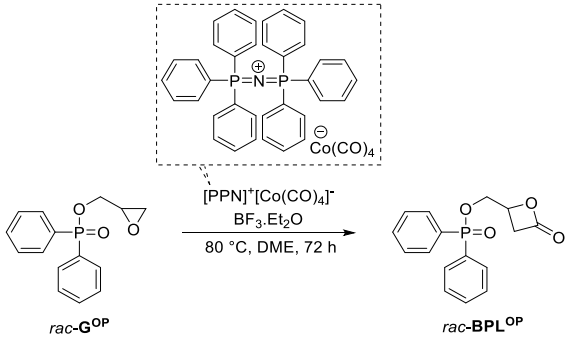


**Scheme 2.** Synthesis of *rac*-BPL$^{OP}$ by carbonylation of the corresponding epoxide *rac*-G$^{OP}$.

observation of two broad resonances in the $^{31}$P{$^1$H} NMR spectrum, a major one ($\delta$ 33.4 ppm) and a minor one ($\delta$ 32.7 ppm) (along the signal at $\delta$ 34.5 ppm for residual monomer; see Figures S10, S12), may possibly reflect the phosphinate moieties in the repeating and terminal (crotonyl) moieties, respectively.

Subsequently, the copolymerization of *rac*-BPL$^{OP}$ with β-butyrolactone (BPL$^{Me}$) was undertaken using deliberately low loadings of the phosphinate comonomer (2–10 mol%); this was aimed at facilitating the global copolymerization, by minimizing the amount of the 'deleterious' phosphinate comonomer, and, at the same time, at preparing P-functionalized PHAs made essentially of poly(3-hydroxybutyrate) (PHB = PBPL$^{Me}$) segments. Two yttrium-based catalysts, known for their different stereoselective abilities, were used to access syndio-enriched (**1a**) or atactic (**1b**) PHB segments; also, a copolymer made of isotactic PHB segments was targeted by using enantiopure (*S*)-BPL$^{Me}$ instead of *rac*-BPL$^{Me}$. The results are summarized in Table 2.

At such low loadings of *rac*-BPL$^{OP}$, complete conversion of both comonomers could be generally reached within 2–3 h at room temperature. The copolymers recovered are readily soluble in chlorinated solvents (dichloromethane, chloroform) and toluene, and very poorly to insoluble in water, alkanes (*n*-pentane, *n*-hexane), ethyl acetate, diethyl ether, and acetone; they could hence be reprecipitated. The amount of BPL$^{OP}$ incorporated within the PHB segments of the P[(BPL$^{Me}$)$_x$-*co*-(BPL$^{OP}$)$_y$] copolymers was assessed by $^1$H NMR analysis of the isolated materials; the values thus determined were matching, in general, quite well the initial comonomer loadings (1.8–8.1 mol% vs. 2–10 mol%, respectively) [50]. The $^1$H and $^{13}$C NMR spectra of the copolymers featured the characteristic resonances of both repeating units (Fig. 1, see also the Supp. Info. Figures S13–S42). The tacticity of the PHB segments was observable at the four different carbon atoms (carbonyl, methine, methylene, methyl; Fig. 2), allowing a fair estimation of the $P_r$ values (probability of racemic enchainment of the BPL$^{Me}$ units) [35,36,51]. As expected using the syndioselective *tert*-butyl substituted catalyst **1a** or the non-selective methyl-substituted catalyst **1b**, copolymers containing syndiotactic-enriched ($P_r$ up to 0.84), atactic ($P_r \sim 0.50$) and highly isotactic ($P_r < 0.06$) PHB segments could be thus prepared. The $^{31}$P{$^1$H} NMR spectra of the various copolymers, no matter their tacticity (and composition), all featured a single sharp resonance at $\delta$ 32.75 ppm (see the Supp. Info., Figures S14, S17, S20, S23, S26, S29), significantly shifted from that of the initial monomer ($\delta$ 33.95 ppm; Figure S5), suggesting a single, isolated environment of the BPL$^{OP}$ units within the macromolecular PHB chains (vide infra).

The presence of α-isopropoxycarbonyl, ω-crotonyl (–C(O)CH = CHCH$_3$) telechelic macromolecular chains could be evidenced both from the $^1$H and $^{13}$C NMR spectra (Fig. 1, see also the Supp. Info., Figures S13–S39) and further supported by 2D $^1$H–$^1$H COSY and $^1$H–$^{13}$C HSQC NMR analyses (Figures S40 and S41). The α-isopropoxycarbonyl end-groups arise from the initiation mediated by the in situ-generated yttrium-isopropoxide species {Y(OiPr){ON(N)O$^{R2}$}, while the ω-crotonyl capping-groups are formed upon termination or transfer reactions from the propagating polymeryl species. The isopropoxycarbonyl-to-crotonyl end-group ratio, as determined from their respective $^1$H NMR integrations, is usually higher than 1:1 (typically ca. 1:0.2–0.5); this indicates that a significant (major) fraction of the PHA (linear) chains bear another type of ω-terminus, which is most likely –C(O)CH$_2$CH(OH)CH$_3$ that cannot be easily identified in the NMR spectra (note that the crotonyl end-group is actually obtained by the formal dehydration of the latter terminal hydroxy moiety). Also, it is important to remind that regular $^1$H or $^{13}$C NMR analyses does not enable to assess the possible presence of cyclic P[(BPL$^{Me}$)$_x$-*co*-(BPL$^{OP}$)$_y$] macromolecules since, per se, they have no end-groups. A DOSY NMR experiment revealed that the diphenylphosphinate moieties arising from the BPL$^{OP}$ comonomer are associated to polymer populations (see Figure S43); yet it did not allow assessing the exact composition of macromolecules, unlike mass spectrometry which provided details (vide infra).

The molar masses of the copolymers were determined from the $^1$H

**Table 1**
ROP of *rac*-BPL$^{OP}$ mediated by the **1a**/*i*PrOH catalyst system.[a]

| Entry | $[BPL^{OP}]_0$[b] (equiv vs. Y) | Temp. (°C) | Reaction time (h) | Conv.[c] $[BPL^{OP}]_0$ (mol%) | $M_{n,theo}$[d] (g.mol$^{-1}$) | $M_{n,NMR}$[e] (g.mol$^{-1}$) | $M_{n,SEC}$[f] (g.mol$^{-1}$) | $Đ_M$[f] |
|---|---|---|---|---|---|---|---|---|
| 1 | 10 | 25 | 42 | 42 | 1350 | 1100 | *n.d.*[g] | *n.d.*[g] |
| | | | 144 | 66 | 2050 | 1750 | 1800 | 1.09 |
| 2 | 30 | 25 | 3 | 38 | 3500 | 2200 | 7000 | 1.32 |
| 3 | 30 | 60 | 3 | 42 | 3900 | 4300 | 6600 | 1.35 |

[a] Reactions performed with $[BPL^{OP}]_0 = 1.0$ M in toluene with [**1a**]/[*i*PrOH]$_0$ = 1:1. [b] Monomer loading. [c] Conversion of BPL$^{OP}$ as determined by $^1$H NMR analysis of the crude reaction mixture. [d] Theoretical molar mass value calculated according to $M_{n,theo} = [BPL^{OP}]_0/[\mathbf{1a}] \times conv.(BPL^{OP}) \times M(BPL^{OP}) + M(i\text{PrOH})$, with $M(BPL^{OP}) = 302$ g.mol$^{-1}$ and $M$(*i*PrOH) = 60 g.mol$^{-1}$. [e] Experimental molar mass value determined by $^1$H NMR analysis of the isolated polymer, from the resonances of the terminal O*i*Pr group (refer to Experimental section). [f] Number-average molar mass (uncorrected values) and dispersity ($M_w/M_n$) as determined by SEC analysis in THF at 30 °C vs. polystyrene standards; [g] Not determined.

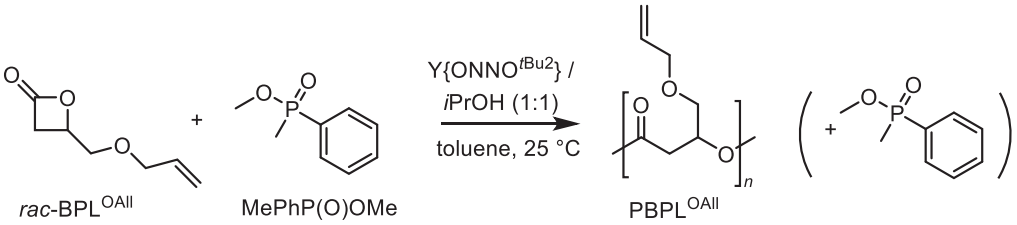


| | | | | |
|---|---|---|---|---|
| 25 equiv | 0 equiv | 1 h, 100% conv | $M_{n,theo}$ = 3600 | $M_{n,NMR}$ = 3500 g mol$^{-1}$ |
| 25 equiv | 25 equiv | 24 h, 19% conv | $M_{n,theo}$ = 1000 | $M_{n,NMR}$ = 1050 g mol$^{-1}$ |
| | | 72 h, 40% conv | $M_{n,theo}$ = 1850 | $M_{n,NMR}$ = 2000 g mol$^{-1}$ |

**Scheme 3.** Control experiments evidencing the deleterious influence of the phosphinate moiety on the activity of the **1a**/*i*PrOH catalyst system on the ROP of *rac*-BPL$^{OAll}$.

**Table 2**
Ring-opening copolymerization of *rac*- or (*S*)-BPL$^{Me}$ with *rac*-BPL$^{OP}$ mediated by Y(N(SiHMe$_2$)$_2$){ONNO$^{R2}$} (**1a-b**)/*i*PrOH catalytic systems and characteristics of the resulting P(BPL$^{Me}$-*co*-BPL$^{OP}$)s.[a]

| Entry | Cat. | $[BPL^{OP}]_0/[BPL^{Me}]_0/[1]_0/[i\text{PrOH}]_0$ | Reaction time[b] (h) | Conv.[c] BPL$^{OP}$/BPL$^{Me}$ (mol%) | BPL$^{OP}$ incorp.[d] (mol%) | $M_{n,theo}$[e] (g. mol$^{-1}$) | $M_{n,NMR}$[f] (g. mol$^{-1}$) | $M_{n,SEC}$[g] (g. mol$^{-1}$) | $Đ_M$[g] | $P_r$[h] PHB block | $T_g$[i] (°C) | $T_m$[i] (°C) | $\Delta H_m$[i] (J. g$^{-1}$) | $T_d^{5\%}$[j] (°C) | $T_d^{80\%}$[j] (°C) |
|---|---|---|---|---|---|---|---|---|---|---|---|---|---|---|---|
| 1 | **1a** | 1:49:1:1 | 2 | 100/100 | 1.8 | 4600 | 4600 | 7100 | 1.71 | 0.84 | −10.1 | 134.1 | 20 | 192 | 273 |
| 2 | **1a** | 2:98:1:1 | 2.5 | 100/100 | 2.4 | 9100 | 8000 | 8300 | 1.95 | 0.77 | −21.1 | 131.2 | 14 | 126 | 271 |
| 3 | **1a** | 4:196:1:1 | 2.5 | 100/94 | 2.3 | 17,300 | 15,000 | 11,900 | 1.80 | 0.81 | −7.6 | 134.6 | 23 | 130 | 289 |
| 4 | **1a** | 2:48:1:1 | 1 | 41/100 | 3.7 | 4500 | 5500 | 6100 | 1.34 | n.d.[l] | n.d.[l] | n.d.[l] | n.d.[l] | n.d.[l] | n.d.[l] |
| 5 | **1a** | 2:48:1:1 | 3 | 100/100 | 4.0 | 5000 | 5150 | 6150 | 1.78 | n.d.[l] | −11.3 | 127.3 | 14 | 214 | 280 |
| 6 | **1a** | 5:45:1:1 | 6 | 100/100 | 7.5 | 5200 | 5050 | 3300 | 1.81 | 0.70 | −12.8 | ~103 | ~1 | 193 | 312 |
| 7 | **1b** | 1:49:1:1 | 3 | 100/100 | 2.4 | 4600 | 4200 | 5650 | 1.74 | 0.52 | −11.6 | n.o.[m] | n.o.[m] | 109 | 275 |
| 8[k] | **1a** | 1:49:1:1[k] | 2 | 100/100 | 2.3 | 4600 | 4600 | 5200 | 1.57 | 0.06[j] | −9.7 | 137.1 | 47 | 227 | 283 |

[a] Reactions performed in toluene at room temperature with $[BPL^{Me}]_0 + [BPL^{OP}]_0 = 1.0$ M. [b] Reaction time, not necessarily optimized. [c] Conversion of BPL$^{OP}$ and BPL$^{Me}$ as determined by $^1$H NMR analysis of the crude reaction mixture. [d] Amount of BPL$^{OP}$ incorporated into PBPL$^{Me}$, as determined by $^1$H NMR on the precipitated copolymer. [e] Theoretical molar mass value calculated according to $M_{n,theo} = ([BPL^{OP}]_0/[1]_0 \times conv.(BPL^{OP}) \times M(BPL^{OP})) + ([BPL^{Me}]_0/[1]_0 \times conv.(BPL^{Me}) \times M(BPL^{Me})) + M(i\text{PrOH})$, with $M(BPL^{OP}) = 302$ g.mol$^{-1}$, $M(BPL^{Me}) = 86$ g.mol$^{-1}$, and $M$(*i*PrOH) = 60 g.mol$^{-1}$. [f] Experimental molar mass determined by $^1$H NMR analysis of the isolated polymer, from the resonances of the terminal O*i*Pr group (refer to Experimental section). [g] Number-average molar mass (uncorrected values) and dispersity ($M_w/M_n$) determined by SEC analysis in $CDCl_3$ at 30 °C vs. polystyrene standards. [h] $P_r$ is the probability of *racemic* linkages between BPL$^{Me}$ units in the PBPL$^{Me}$ block, as determined by $^{13}C\{^1H\}$ NMR analysis of the isolated copolymer. [i] Glass transition temperature, melting temperature and melting enthalpy as determined by DSC. [j] Degradation temperature at 5% and 80% weight loss, as determined by TGA. [k] Enantiopure (*S*)-BPL$^{Me}$. [l] Not determined. [m] No melting transition observed.

NMR spectra considering the α-isopropoxycarbonyl end-group resulting from the initiation step (see the Experimental section for calculation details). The $M_{n,NMR}$ values thus determined were in good agreement with the $M_{n,theo}$ values calculated from the monomer-to-initiator ratio and the monomers' conversion (Table 2). The $M_{n,SEC}$ values determined in chloroform relative to polystyrene standards (values uncorrected for possible differences in hydrodynamic radii) roughly followed the same trend. More importantly, the dispersity values determined by SEC ($Đ_M$ = $M_w/M_n$ = 1.34–1.95) were significantly larger than those of PHB homopolymers prepared from the ROP of *rac*- or enantiopure-BPL$^{Me}$ under similar conditions ($Đ_M < 1.3$) [35,36]. We assume that this broadening reflects competitive initiation vs. propagation in the presence of the BPL$^{OP}$ monomer, likely because of the aforementioned coordination of the phosphinate moiety onto the yttrium center of the catalyst/initiator which competes with that of the β-lactones.

To get a better insight into the microstructure of the P(BPL$^{Me}$-*co*-

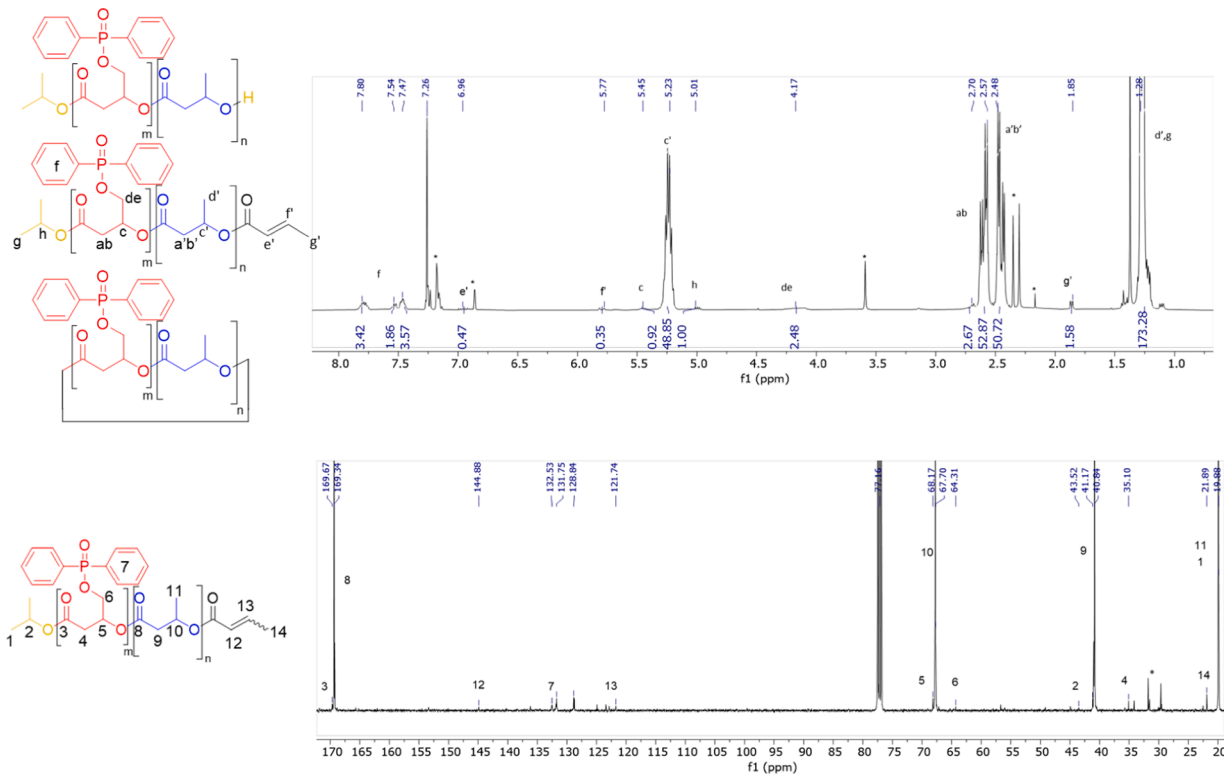


**Fig. 1.** Representative $^{1}$H (top; 400 MHz, $CDCl_3$, 25 °C) and $^{13}C\{^{1}H\}$ (bottom; 125 MHz, $CDCl_3$, 25 °C) NMR spectra of a P(BPL$^{Me}$-*co*-BPL$^{OP}$) sample prepared from the ROCOP of *rac*-BPL$^{Me}$ and *rac*-BPL$^{OP}$ mediated by the **1a**/*i*PrOH (1:1) catalyst system (Table 1, entry 1), depicting the cyclic and linear copolymers observed. * stands for resonances of residual solvent and/or catalyst.

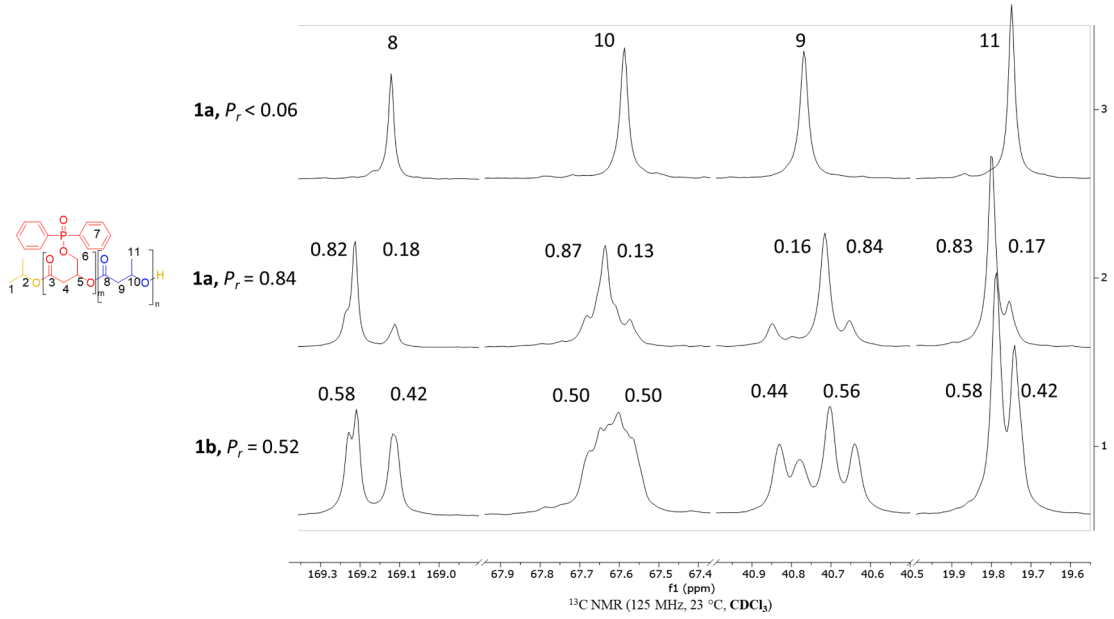


**Fig. 2.** Regions of the $^{13}C\{^{1}H\}$ NMR spectra (125 MHz, $CDCl_3$, 23 °C) of P(BPL$^{Me}$-*co*-BPL$^{OP}$) samples, showing the tacticity of PHB segments, prepared by ROCOP of *rac*-BPL$^{OP}$ with: enantiopure (*S*)-BPL$^{Me}$ (top spectrum; Table 1, entry 8), *rac*-BPL$^{Me}$ (middle spectrum; Table 1, entry 1), and *rac*-BPL$^{Me}$ (bottom spectrum; Table 1, entry 7), mediated by **1a**, **1a**, and **1b**/*i*PrOH, respectively.

BPL$^{OP}$) copolymers produced and to demonstrate the effective incorporation of BPL$^{OP}$ units within the PHB macromolecular chains, mass spectrometric analyses were conducted. Matrix-assisted laser desorption ionization time-of-flight (MALDI-ToF) mass spectrometry analysis, which enables studying more easily high molar mass materials than electrospray ionization (ESI), relatively, returned mass spectra featuring normal distributions over a large range of *m/z* values. Two representative examples of such MALDI-ToF mass spectra are given in Fig. 3a. The two most intense distributions observed in both cases (the relative intensity of which differs from one to another sample) were identified (from high-resolution ESI mass spectra – Fig. 3b), as on one hand, the linear *i*PrO-[P(BPL$^{Me}$)$_x$-*co*-(BPL$^{OP}$)$_y$]-H series, and, on the other hand,

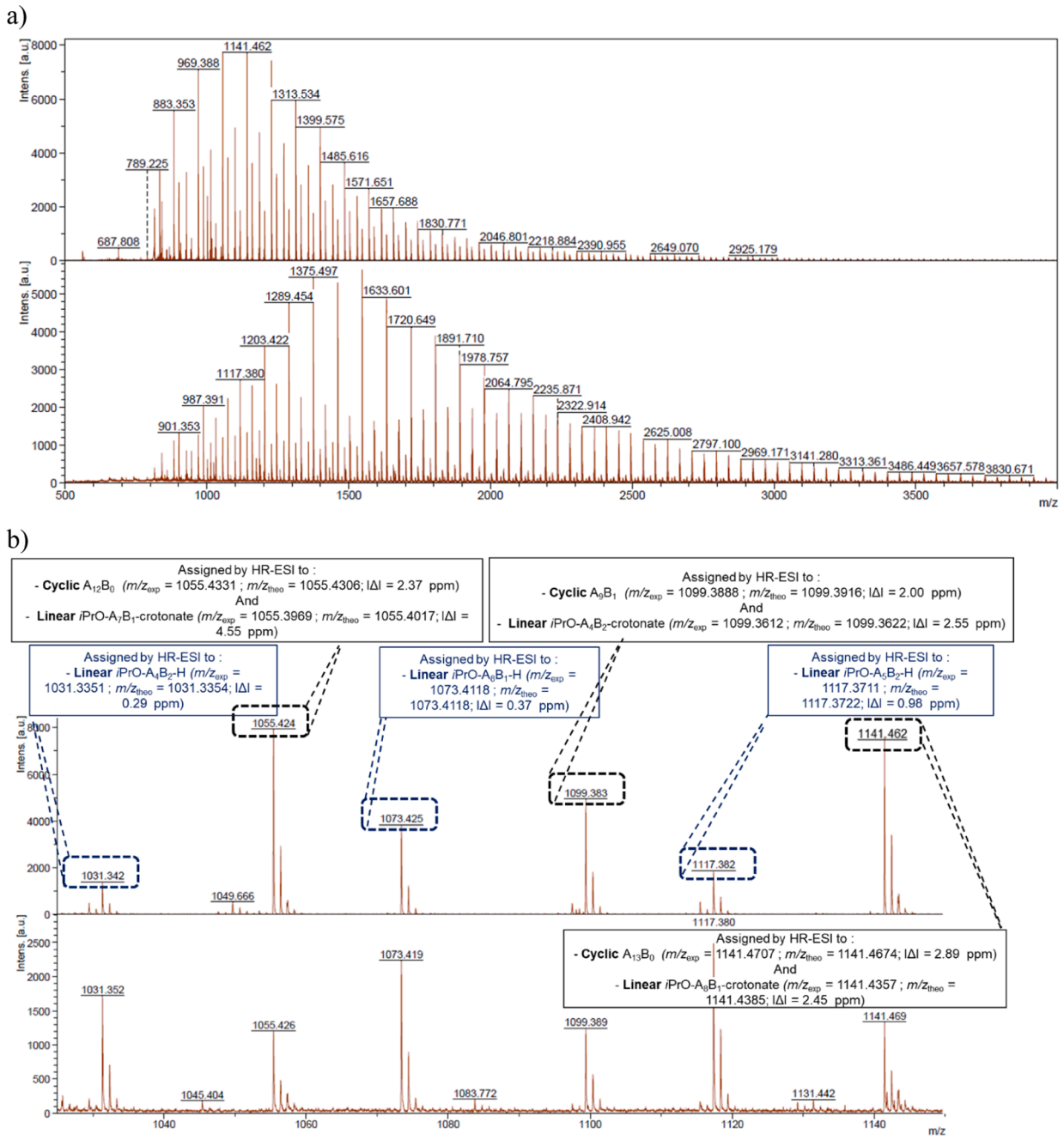


**Fig. 3.** Mass spectra (DCTB matrix, ionized by $Na^+$) of P(BPL$^{Me}$-*co*-BPL$^{OP}$) samples prepared by ROCOP of *rac*-BPL$^{Me}$ and *rac*-BPL$^{OP}$ mediated by the **1a**/*i*PrOH catalyst system (top spectra: Table 1, entry 5; bottom spectra, entry 4): (a) MALDI-ToF mass spectra for $m/z$ up to 4000, (b) zoomed region ($m/z$ = 1025–1150) of the two above mass spectra, respectively, with corresponding assignments of the two major series observed, as determined from high-resolution (HR) ESI mass spectra (see Fig. 4 and Figure S68-S71) [52]; for the sake of clarity in the assigned compositions, A and B stand for BPL$^{Me}$ and BPL$^{OP}$ units, respectively.

the cyclic [P(BPL$^{Me}$)$_x$-*co*-(BPL$^{OP}$)$_y$] and the crotonate-terminated *i*PrO-[P(BPL$^{Me}$)$_x$-*co*-(BPL$^{OP}$)$_y$]–(C(O)CH=CHCH$_3$) series, which overlap in the MALDI-ToF mass spectra.

Distinction and clear authentication of the latter two series was only possible by high-resolution (HR) ESI-MS (Fig. 4 and Figures S68–S71) [52]. Assignments of the different series were confirmed by comparison of theoretical mass values calculated for a variety of compositions (i.e. number of BPL$^{Me}$ (referred to as "A") and BPL$^{OP}$ (referred to as "B") units, $x$ = 1–15 and $y$ = 0–2, respectively, with either a macrocyclic structure or a variety of terminal groups for linear populations) with the experimental $m/z$ values determined by HR-ESI MS (see the Supp. Info., Table S2). This enabled to plot the distributions of each individual polymer series experimentally observed for a given HR-ESI MS analysis of a copolymer sample. An example of such a plot is given in Fig. 5. It features essentially the three major series of macromolecules, that is the cyclic one and the linear ones with an α-isopropoxy group and, on the other terminus, either an ω-hydroxy or a ω-crotonate end-group [53,54,55]. For each of these series, the populations containing $y$ = 0, 1 or 2 BPL$^{OP}$ units were unambiguously distinguished. Of course, caution must be taken in analyzing the relative intensities of these populations because ESI can discriminate between lower and larger $m/z$ values (i.e., the distributions could be different than what is observed in the spectra in the shorter and longer macromolecules, the latter ones being unobserved for most of them) and also, because the presence of phosphonate moieties could affect (favorably or not) the ionization process. Yet, it is noteworthy that these nine distinct series all feature

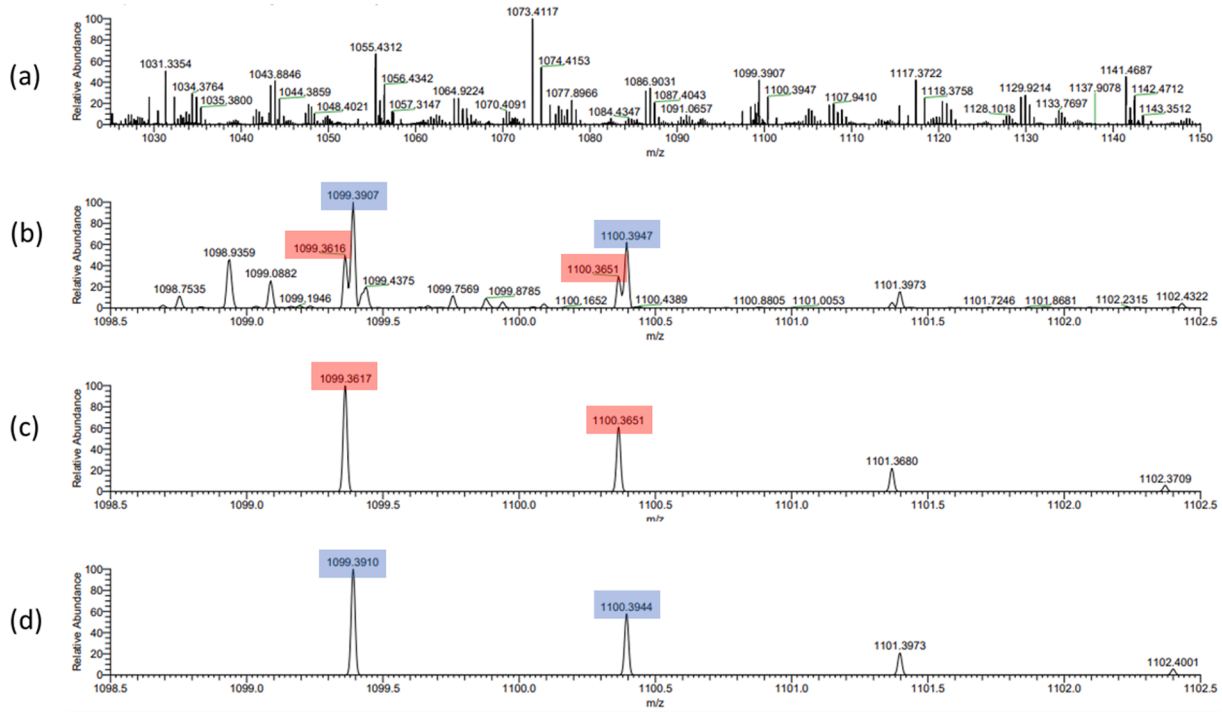


**Fig. 4.** Details of the high-resolution ESI mass spectrum (MeOH) of a P(BPL$^{Me}$-*co*-BPL$^{OP}$) sample prepared by ROCOP of *rac*-BPL$^{Me}$ and *rac*-BPL$^{OP}$ mediated by the **1a**/*i*PrOH catalyst system (Table 1, entry 5), from top to bottom: (a) experimental spectrum for $m/z$ = 1025–1150, (b) zoomed region for $m/z$ = 1098.5–1102.5, showing resolved peaks for cyclic [P(BPL$^{Me}$)$_9$-*co*-(BPL$^{OP}$)$_1$] ($m/z_{exp}$ (all $^{12}$C) = 1099.3907) and *i*PrO-[P(BPL$^{Me}$)$_4$-*co*-(BPL$^{OP}$)$_2$]–(C(O)CH=CHCH$_3$) ($m/z_{exp}$ (all $^{12}$C) = 1099.3616); (c) calculated spectrum (isotopic pattern) for *i*PrO-[P(BPL$^{Me}$)$_4$-*co*-(BPL$^{OP}$)$_2$]–(C(O)CH=CHCH$_3$) ($m/z_{calcd}$ (all $^{12}$C) = 1099.3617) [53]; (d) calculated spectrum (isotopic pattern) for cyclic [P(BPL$^{Me}$)$_9$-*co*-(BPL$^{OP}$)$_1$] ($m/z_{calcd}$ (all $^{12}$C) = 1099.3910).

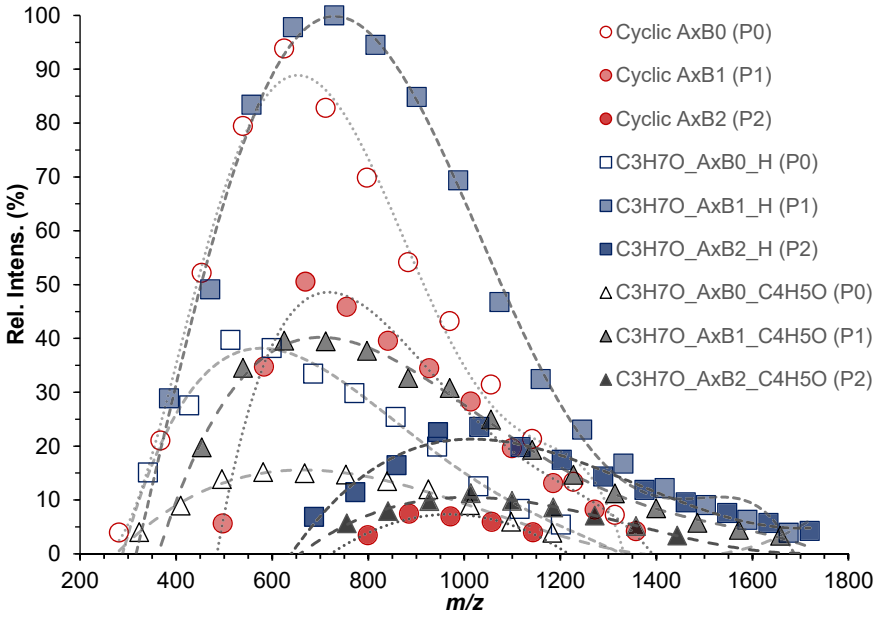


**Fig. 5.** Distribution of individual polymer series experimentally observed in the high-resolution ESI MS analysis (MeOH, Fig. 4) of a copolymer sample prepared by ROCOP of *rac*-BPL$^{Me}$ and *rac*-BPL$^{OP}$ mediated by **1a**/*i*PrOH catalyst system (Table 1, entry 5). Three major series of macromolecules, that is cyclic [P(BPL$^{Me}$)$_x$-*co*-(BPL$^{OP}$)$_y$] (○) and linear *i*PrO-[P(BPL$^{Me}$)$_x$-*co*-(BPL$^{OP}$)$_y$]–H (□) and *i*PrO-[P(BPL$^{Me}$)$_x$-*co*-(BPL$^{OP}$)$_y$]–(C(O)CH=CHCH$_3$) (Δ) [52] containing each 0, 1 or 2 BPL$^{OP}$ units, are distinguished.

"normal/Gaussian" distributions, which indicates that an even detection of the different, short and long macromolecules they are made of, was eventually achieved. Also, it could be noted that for the linear (ω-hydroxyl- or ω-crotonate-terminated) chains, those containing one BPL$^{OP}$ moiety ($B_1$) are more abundant than those having none or two such phosphinate comonomer unit(s) ($B_0$, $B_2$) (see Fig. 3b and 5). Conversely, the cyclic homo-PHB population is apparently more abundant than the two cyclic copolymer ones containing, respectively, one and two BPL$^{OP}$ moieties. This can be tentatively rationalized considering that cyclic macromolecules are formed via 'back-biting' (i.e. intramolecular

transesterification) of the *i*PrO-[P(BPL$^{Me}$)$_x$-*co*-(BPL$^{OP}$)$_y$]-H chains; since, as aforementioned, the most abundant latter series contains a single BPL$^{OP}$ unit ($y = 1$), chances to form cyclic macromolecules void of any phosphinate monomer unit are high.

Beyond confirming the effective incorporation of BPL$^{OP}$ unit(s) within PHB macromolecules, these HR-ESI MS data further enable evaluating the ratio between ω-hydroxy and ω-crotonate end-group from the relative intensities of these two series in the mass spectra. In a given sample, it proved relatively similar among the different set of macromolecules with variable $x/y$ values, and the average ratio thus evaluated for the whole population of macromolecules detected by ESI-MS (ca. 60–70 % ω-OH, 30–40 % ω-crotonate for entry 5, Fig. 5 and Table S2) proved similar to that determined by $^1$H NMR (ca. 60:40; see Figure S25).

The thermal signature of the copolymers was investigated by DSC and TGA (Table 2, Figs. 6-8, Figs. S48-S67). They were also compared with those of 'pristine' PHB homopolymers prepared with the same catalyst under similar conditions (Table S3).

Most copolymers feature a glass transition temperature in the –13 to –7 °C range (Table 2), somewhat similar to that of PBL$^{Me}$ homopolymers. Also, most copolymers retain a semi-crystalline character with melting transition temperatures in the range 127 to 135 °C (syndiotactic) and 137 °C (isotactic), which is slightly lower to that of pristine PBL$^{Me}$ homopolymers ($T_m$ = ca. 140 °C for syndiotactic and ca. 147/170 °C for isotactic), as expected from the introduction of a comonomer.

The influence of the phosphinate content in the copolymer on the thermal decomposition (TGA) under nitrogen was assessed with materials having similar syndiotacticity and molar mass (Fig. 6). The onset decomposition temperature ($T_d^{5\%}$) did not vary much between the three copolymer samples (192–214 °C), but it was lower than that of pristine PHB (236 °C). On the other hand, the more phosphinate in the materials, the larger the residue (a black tar) at high temperature ($T > 300$ °C) with the 7.5 mol% copolymer clearly standing out (i.e., residue at 450 °C = 5.5, 8.7, 10.3 and 15.3 wt% for 0, 1.8, 4.0 and 7.5 mol% of BPL$^{OP}$, respectively).

Copolymers with similar molar mass and BPL$^{OP}$ content (1.8–2.4 mol %) but with a different tacticity, featured also a differentiated thermal behavior (Fig. 7 Fig. S65b). The onset decomposition temperature of the atactic material was much lower than those of the syndio-enriched and isotactic copolymers ($T_d^{5\%}$ = 109 °C vs. 192 and 227 °C, $T_d^{10\%}$ = 158 °C vs. 217 and 240 °C, $T_d^{20\%}$ = 234 °C vs. 239 and 254 °C, respectively). Also, the isotactic copolymer revealed thermally more stable at higher temperature than the other two copolymers ($T_{asymp}$ = 273 °C vs. 264 and 267 °C, for $P_r$ = 0.06 vs. 0.84 and 0.52, respectively). As anticipated, the molar mass of the copolymers also affected their thermal behavior; this

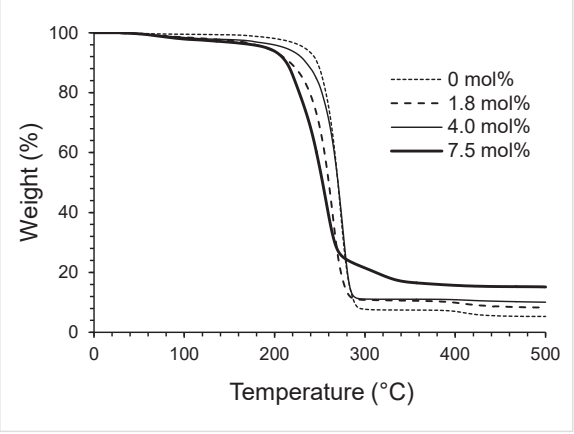


**Fig. 6.** TGA thermograms of a homo PHB (Table S3) and of P(BPL$^{Me}$-*co*-BPL$^{OP}$) samples with different % of BPL$^{OP}$ incorporated within the PHB backbone (Table 2, entries 1/5/6).

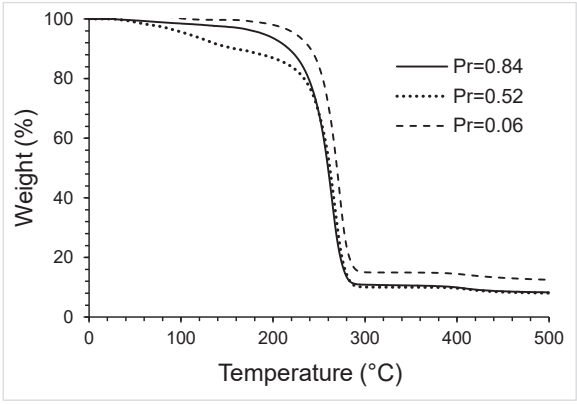


**Fig. 7.** TGA thermograms of P(BPL$^{Me}$-*co*-BPL$^{OP}$) samples with different tacticities of the PHB block (Table 2, entries 1/7/8).

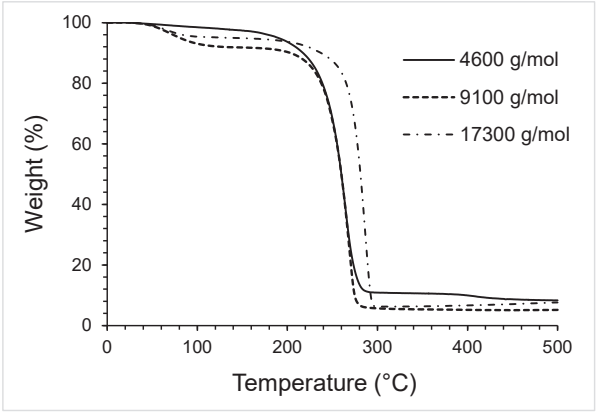


**Fig. 8.** TGA thermograms of P(BPL$^{Me}$-*co*-BPL$^{OP}$) samples with different average molecular masses (Table 2, entries 1/2/3).

was assessed by comparison of three syndio-enriched samples with similar BPL$^{OP}$ content (1.8–2.4 mol%) prepared by increasing the [BPL$^{OP}$]$_0$/[BPL$^{Me}$]$_0$/[**1a**]$_0$/[*i*PrOH]$_0$ feed ratio from 1:49:1:1, to 2:98:1:1 and 4:196:1:1 (Table 2, entries 1, 2 and 3; Fig. 8 and Fig. S66b). Although these three polymer materials had essentially the same residue at $T > 300$ °C (ca. 10 wt%), the one with the larger molar mass showed, as anticipated, a clear delayed decomposition as compared to the other two shorter ones ($T_d^{20\%}$ = 265 °C vs. 239 and 238 °C, and $T_{asymp}$ = 286 °C vs. 264 and 269 °C, for $M_{n,NMR}$ = 15,000 vs. 4600 and 8000 g.mol$^{-1}$, respectively). One can thus tune the thermal profile of a P(BPL$^{Me}$-*co*-BPL$^{OP}$) sample upon modifying, beyond the molar mass, the microstructure (i.e. tacticity) and the extent of BPL$^{OP}$ incorporated along the PHB backbone.

## 5. Conclusions

Despite the detrimental influence of the phosphinate moiety on the catalyst activity, effective copolymerization of β-butyrolactone with BPL$^{OP}$, a phosphinate-functionalized β-lactone, could be achieved with yttrium-based catalyst systems. Copolymers constituted of one or several phosphinate moieties within the PBL$^{Me}$ (PHB) macromolecular chains, with controlled molar mass and narrow dispersities, were thus synthesized, as established by different analytical techniques. Mass spectrometric studies proved particularly helpful at elucidating and understanding the nature of the various populations formed, and evidencing the incorporation of the phosphinate-functionalized β-lactone.

These copolymers constitute novel examples of phosphorus-modified

PHAs with various tacticities (isotactic, syndiotactic, atactic), topology (linear, cyclic) that can be tuned either by the enantiopurity of the monomers or starting from racemic monomers via adjusting the nature of the yttrium catalyst systems at play. These results illustrate how PHBs can be chemically modified upon incorporation of as little as 10 % of a phosphinate substituent throughout its backbone, by the ROCOP approach. Furthermore, this strategy enabled to modulate the thermal signature of the thus phosphinated PHB.

## CRediT authorship contribution statement

**Ali Dhaini:** Investigation, Formal analysis, Writing – original draft, Writing – review & editing. **Rama M. Shakaroun:** Investigation, Formal analysis, Writing – original draft, Writing – review & editing. **Jérôme Ollivier:** Mass spectrometry analysis, formal analysis, Data curation, Writing – review & editing. **Ali Alaaeddine:** Supervision. **Sophie M Guillaume:** Writing – review & editing, Writing – original draft, Supervision, Formal analysis, Conceptualization. **Jean-François Carpentier:** Writing – review & editing, Writing – original draft, Supervision, Formal analysis, Conceptualization.

## Declaration of competing interest

The authors declare that they have no known competing financial interests or personal relationships that could have appeared to influence the work reported in this paper.

## Data availability

Data will be made available on request.

## Acknowledgments

This research was financially supported in part by the University of Rennes (Ph.D. grants to R.S. and A.D.) and the Lebanese University (Ph. D. grants to R.S. and A.D.). We are grateful to CRMPO and UAR Scan-MAT (CNRS, Univ. Rennes), especially to Philippe Jéhan, Nicolas Le Yondre and Elsa Caytan, for MS and NMR analyses, respectively. We thank Maxime Lanvin for development of the MS data-processing script. We thank Thierry Roisnel (ISCR, Centre de diffraction) for solving the X-ray structure of BPLOP.

## Appendix A. Supplementary data

Supplementary data to this article can be found online at https://doi.org/10.1016/j.eurpolymj.2024.112919.

## References

[1] M. Koller (Ed.) The Handbook of polyhydroxyalkanoates, V1-3, CRC Press (1st ed.) 2020.
[2] Z.A. Raza, S. Abid, I.M. Banat, Polyhydroxyalkanoates: characteristics, production, recent developments and applications, Int. Biodeterio. Biodegrad. 126 (2018) 45–56, https://doi.org/10.1016/j.ibiod.2017.10.001.
[3] R. Muthuraj, O. Valerio, T.H. Mekonnen, Recent developments in short- and medium-chain- length polyhydroxyalkanoates: production, properties, and applications, Int. J. Biol. Macromol. 187 (2021) 422–440, https://doi.org/10.1016/j.ijbiomac.2021.07.143.
[4] S. Taguchi, T. Iwata, H. Abe, Y. Doi, Poly(hydroxyalkanoate)s, in: K. Matyjaszewski, M. Möller (Eds.), Polym. Sci. A Compr. 2020 pp. 157–182.
[5] M. Koller, A. Mukherjee, Polyhydroxyalkanoates – linking properties, applications, and end-of-life options, Chem. Biochem. Eng. 3 (2020) 115–29, 10.15255/CABEQ.2020.1819.
[6] A. Dhaini, V. Hardouin-Duparc, A. Alaaeddine, J.-F. Carpentier, S.M. Guillaume, Recent advances in polyhydroxyalkanoates degradation and chemical recycling, Prog. Polym. Sci. 149 (2024) 101781, https://doi.org/10.1016/j.progpolymsci.2023.101781.
[7] V.V. Andhalkar, R. Ahorsu, P. Domínguez de María, J. Winterburn, F. Medina, M. Constantí, Valorization of lignocellulose by producing polyhydroxyalkanoates under circular bioeconomy premises: facts and challenges, ACS Sustain. Chem. Eng. 10 (2022) 16459–16475, https://doi.org/10.1021/acssuschemeng.2c04925.
[8] B. Dalton, P. Bhagabati, J. De Micco, R.B. Padamati, K. O'Connor, A review on biological synthesis of the biodegradable polymers polyhydroxyalkanoates and the development of multiple applications, Catalyst 13 (2022) 319, https://doi.org/10.3390/catal12030319.
[9] A. Anjum, M. Zuber, K.M. Zia, A. Noreen, M.N. Anjum, S. Tabasum, Microbial production of polyhydroxyalkanoates and its copolymers: a review of recent advancements, Int. J. Biol. Macromol. 89 (2016) 161–174, https://doi.org/10.1016/j.ijbiomac.2016.04.069.
[10] B. Laycock, P. Halley, S. Pratt, A. Werker, P. Lant, The chemomechanical properties of microbial polyhydroxyalkanoates, Prog. Polym. Sci. 38 (2013) 536–583, https://doi.org/10.1016/j.progpolymsci.2012.06.003.
[11] P. Dubois, O. Coulembier, J.-M. Raquez, Handbook of ring-opening polymerization, Wiley, Weinheim, 2009. For leading reviews on stereoselective metal-catalyzed ROP of lactones and related derivatives, see:.
[12] M.J. Stanford, A.P. Dove, Stereocontrolled ring-opening polymerisation of lactide, Chem. Soc. Rev. 39 (2010) 486–494, https://doi.org/10.1039/B815104K.
[13] P.J. Dijkstra, H. Du, J. Feijen, Single site catalysts for stereoselective ring-opening polymerization of lactides, Polym. Chem. 2 (2011) 520–527, https://doi.org/10.1039/C0PY00204F.
[14] A. Buchard, C.M. Bakewell, J. Weiner, C.K. Williams, Recent developments in catalytic activation of renewable resources for polymer synthesis, Top. Organomet. Chem. 39 (2012) 175–224, https://doi.org/10.1007/978-3-642-28288-1_5.
[15] S.M. Guillaume, E. Kirillov, Y. Sarazin, J.-F. Carpentier, Beyond stereoselectivity, switchable catalysis: some of the last frontier challenges in ring-opening polymerization of cyclic esters, Chem. Eur. J. 21 (2015) 7988–8003, https://doi.org/10.1002/chem.201500613.
[16] J.C. Worch, H. Prydderch, S. Jimaja, P. Bexis, M.L. Becker, A.P. Dove, Stereochemical enhancement of polymer properties, Nature Rev. Chem. 3 (2019) 514–535, https://doi.org/10.1038/s41570-019-0117-z.
[17] M.-J.-L. Tschan, R.M. Gauvin, C.M. Thomas, Controlling polymer stereochemistry in ring-opening polymerization: a decade of advances shaping the future of biodegradable polyesters, Chem. Soc. Rev. 50 (2021) 13587–13608, https://doi.org/10.1039/D1CS00356A.
[18] L. Al-Shok, D.M. Haddleton, F. Adams, Progress in catalytic ring-opening polymerization of biobased lactones, in: A. Kunkel, G. Battagliarin, M. Winnacker, B. Rieger, G. Coates (Eds.), Advances in Polymer Science, Springer, 2022, pp. 197–267.
[19] A.H. Westlie, E.C. Quinn, C.R. Parker, E.-Y.-X. Chen, Synthetic biodegradable polyhydroxyalkanoates: recent advances and future challenges, Prog. Polym. Sci. 134 (2022) 101608, https://doi.org/10.1016/j.progpolymsci.2022.101608.
[20] Z. Zhang, C. Shi, M. Scoti, X. Tang, E.-Y.-X. Chen, Alternating isotactic polyhydroxyalkanoates via site- and stereoselective polymerization of unsymmetrical diolides, J. Am. Chem. Soc. 144 (2022) 20016–20024, https://doi.org/10.1021/jacs.2c08791.
[21] J.-F. Carpentier, Rare earth complexes supported by tripodal tetradentate bis (phenolate) ligands: a privileged class of catalysts for ring-opening polymerization of cyclic esters, Organometallics 34 (2015) 4175–4189, https://doi.org/10.1021/acs.organomet.5b00540.
[22] R.M. Shakaroun, A. Dhaini, R. Ligny, A. Alaaeddine, S.M. Guillaume, J.-F. Carpentier, Stereo-electronic contributions in yttrium-mediated stereoselective ring-opening polymerization of functional racemic β-lactones: ROP of 4-alkoxymethylene-β-propiolactones with bulky exocyclic chains, Polym. Chem. 14 (2023) 720–727, https://doi.org/10.1039/D2PY01573K.
[23] G. Becker, F.R. Wurm, Functional biodegradable polymers via ring-opening polymerization of monomers without protective groups, Chem. Soc. Rev. 14 (2018) 7739–7782, https://doi.org/10.1039/C8CS00531A.
[24] H. Li, R.M. Shakaroun, S.M. Guillaume, J.-F. Carpentier, Recent advances in metal-mediated stereoselective ring-opening polymerization of functional cyclic esters towards well-defined poly(hydroxy acid)s: from stereoselectivity to sequence-control, Chem. Eur. J. 26 (2020) 128–138, https://doi.org/10.1002/chem.201904108.
[25] R. Ligny, S.M. Guillaume, J.-F. Carpentier, Yttrium-mediated ring-opening copolymerization of oppositely-configurated 4-alkoxymethylene-β-propiolactones. effective access to highly alternated isotactic functional PHAs, Chem. Eur. J. 25 (2019) 6412–6424, https://doi.org/10.1002/chem.201900413.
[26] K.D. Troev, Chemistry and application of H-phosphonates, 1st ed., Elsevier., ISBN: 9780444527370; eBook ISBN: 9780080476490, 2006.
[27] C. Azuma, K. Sanui, K. Koshiishi, N. Ogata, Phosphonylation of an unsaturated polyester, J. Polym. Sci. Polym. Chem. 17 (1979) 287–291, https://doi.org/10.1002/pol.1979.170170130.
[28] C.S. Wang, C.H. Lin, Synthesis and properties of phosphorus-containing PEN and PBN copolyesters, Polymer 40 (1999) 747–757, https://doi.org/10.1016/S0032-3861(98)00288-2.
[29] S.V. Levchik, E.D. Weil, Flame retardancy of thermoplastic polyesters: a review of the recent literature, Polym. Int. 54 (2005) 11–35, https://doi.org/10.1002/pi.1663.
[30] S.-C. Yang J.P. Kim Flame-retardant polyesters. II. Polyester polymers J. Appl. Polym. Sci. 106 2007 1274 1280 10.1002/app.26544.
[31] S. Brehme, B. Schartel, J. Goebbels, O. Fischer, D. Pospiech, Y. Bykov, M. Döring, Phosphorus polyester versus aluminium phosphinate in poly(butylene terephthalate) (PBT): Flame retardancy performance and mechanisms, Polym. Degrad. Stab. 96 (2011) 875e884, 10.1016/j.polymdegradstab.2011.01.035.
[32] F. Sinclair, L. Chen, B.W. Greenland, M.P. Shaver, Installing multiple functional groups on biodegradable polyesters via post-polymerization olefin cross-metathesis, Macromolecules 49 (2016) 6826–6834, https://doi.org/10.1021/acs.macromol.6b01571.

[33] L. Al-Shok, J.S. Town, D. Coursari, P. Wilson, D.M. Haddleton, Post-polymerisation modification of poly(3-hydroxybutyrate) (PHB) using thiol–ene and phosphine addition, Polym. Chem. 14 (2023) 2734–2741, https://doi.org/10.1039/D3PY00272A.

[34] L. Ju, J. Pretelt, T. Chen, J.M. Dennis, K.V. Heifferon, D.G. Baird, T.E. Long, R. B. Moore, Synthesis and characterization of phosphonated poly(ethylene terephthalate) ionomers, Polymer 151 (2018) 154–163, https://doi.org/10.1016/j.polymer.2018.07.065. For the synthesis of phosphonated poly(ethylene terephthalate) ionomers via polycondensation of (5-disodiumphosphonate) isophtalate with ethyleneglycol, see:.

[35] A. Amgoune, C.M. Thomas, S. Ilinca, T. Roisnel, J.-F. Carpentier, Highly active, productive, and syndiospecific yttrium initiators for the polymerization of racemic β-butyrolactone, Angew. Chem. Int. Ed. 45 (2006) 2782–2784, https://doi.org/10.1002/anie.200600058.

[36] M. Bouyahyi, N. Ajellal, E. Kirillov, C.M. Thomas, J.-F. Carpentier, Exploring electronic versus steric effects in stereoselective ring-opening polymerization of lactide and β-butyrolactone with amino-alkoxy-bis(phenolate)-yttrium complexes, Chem. Eur. J. 17 (2011) 1872–1883, https://doi.org/10.1002/chem.201002779.

[37] J.W. Kramer, E.B. Lobkovsky, G.W. Coates, Practical β-lactone synthesis: epoxide carbonylation at 1 atm, Org. Lett. 8 (2006) 3709–3712, https://doi.org/10.1021/ol061292x.

[38] S.E. Schaus, B.D. Brandes, J.F. Larrow, M. Tokunaga, K.B. Hansen, A.E. Gould, M. E. Furrow, E.N. Jacobsen, Highly selective hydrolytic kinetic resolution of terminal epoxides catalyzed by chiral (salen)CoIII complexes. practical synthesis of enantioenriched terminal epoxides and 1,2-diols, J. Am. Chem. Soc. 124 (2002) 1307–1315, https://doi.org/10.1021/ja016737l.

[39] H.V. Babu, K. Muralidharan, Polyethers with phosphate pendent groups by monomer activated anionic ring opening polymerization: syntheses, characterization and their lithium-ion conductivities, Polymer 55 (2014) 83–94, https://doi.org/10.1016/j.polymer.2013.12.005.

[40] J.T. Lee, P. Thomas, H. Alper, Synthesis of β-lactones by the regioselective, cobalt and Lewis acid catalyzed carbonylation of simple and functionalized epoxides, J. Org. Chem. 66 (2001) 5424–5426, https://doi.org/10.1021/jo010295e.

[41] Y.D. Getzler, V. Mahadevan, E.B. Lobkovsky, G.W. Coates, Synthesis of β-lactones: a highly active and selective catalyst for epoxide carbonylation, J. Am. Chem. Soc. 124 (2002) 1174–1175, https://doi.org/10.1021/ja017434u.

[42] V. Mahadevan, Y.D. Getzler, G.W. Coates, [Lewis Acid]+Co(CO)4− complexes: a versatile class of catalysts for carbonylative ring expansion of epoxides and aziridine, Angew. Chem. Int. Ed. 41 (2002) 2781–2784, https://doi.org/10.1002/1521-3773(20020802)41:15%3C2781::aid-anie2781%3E3.0.co;2-s.

[43] J.A. Schmidt, V. Mahadevan, Y.D. Getzler, G.W. Coates, A readily synthesized and highly active epoxide carbonylation catalyst based on a chromium porphyrin framework: expanding the range of available β-lactones, Org. Lett. 6 (2004) 373–376, https://doi.org/10.1021/ol036244g.

[44] J.A. Schmidt, E.B. Lobkovsky, G.W. Coates, Chromium (III) octaethylporphyrinato tetracarbonylcobaltate: a highly active, selective, and versatile catalyst for epoxide carbonylation, J. Am. Chem. Soc. 127 (2005) 11426–11435, https://doi.org/10.1021/ja051874u.

[45] J.W. Kramer, G.W. Coates, Fluorinated β-lactones and poly(β-hydroxyalkanoate)s: synthesis via epoxide carbonylation and ring-opening polymerization, Tetrahedron 64 (2008) 6973–6978, 10.1016%2Fj.tet.2008.03.108.

[46] Coord. Chem. Rev. 340 (2017) 62–78, https://doi.org/10.1016/j.ccr.2016.09.012.

[47] P.E. Sues, A.J. Lough, R.H. Morris, Synthesis, characterization, and activity of Yttrium(III) nitrate complexes bearing tripodal phosphine oxide and mixed phosphine–phosphine oxide ligands, Inorg. Chem. 51 (2012) 9322–9332, https://doi.org/10.1021/ic3010147.

[48] K.C. Casey, A.M. Brown, J.R. Robinson, Yttrium and lanthanum bis(phosphine-oxide)methanides: structurally diverse, dynamic, and reactive, Inorg. Chem. Front. 8 (2021) 1539–1552, https://doi.org/10.1039/D0QI01438A.

[49] R. Ligny, M.M. Hänninen, S.M. Guillaume, J.-F. Carpentier, Highly syndiotactic or isotactic polyhydroxyalkanoates by ligand-controlled yttrium-catalyzed stereoselective ring-opening polymerization of functional racemic β-lactones, Angew. Chem. Int. Ed. 56 (2017) 10388–10393, https://doi.org/10.1002/anie.201704283.

[50] For entry 6, the experimental value of incorporated $BPL^{OP}$ comonomer is somewhat lower than that expected (7.5 vs 10.0 mol%). Note that these values were determined on reprecipitated polymer and not on the crude material, and since yields of copolymers recovered from reprecipitation were not quantitative (i.e., in the 70-80% range), this may account for the observed differences. Also, the accuracy of the $^1$H NMR determination is evaluated to ± 0.5%.

[51] J.E. Kemnitzer, S.P. McCarthy, R.A. Gross, Preparation of predominantly syndiotactic poly(β-hydroxybutyrate) by the tributyltin methoxide catalyzed ring-opening polymerization of racemic 3-butyrolactone, Macromolecules 26 (1993) 1221–1229, https://doi.org/10.1021/ma00058a004.

[52] The other less intense series observed in the MALDI-ToF mass spectra (e.g. signals observed at $m/z$ = 1045.404, 1083.772, 1131.442; Figure 3b) could not be identified; note that they were not observed in the ESI mass spectra and may therefore result from specific reactions induced by the DCTB matrix. They do not correspond to series of $P(BPL^{OP})_x$-*co*-$(BPL^{Me})_y$ macromolecules bearing α,ω-HO/H, -$(Me_2HSi)_2$N/H, or -$H_2$N/H termini groups (which could have resulted from incidental hydrolysis of terminal/functional groups in the mass spectrometric analysis and/or initiation $(Me_2HSi)_2$N–Y), neither to cyclic or linear macromolecule populations having a $BPL^{OP}$ unit in which the phosphinate moiety would have been hydrolyzed to a $BPL^{OH}$ unit.

[53] Note that linear populations α-*i*PrO,ω–(C(O)CH=$CHCH_3$)-[$P(BPL^{Me})_{x-1}$-*co*-$(BPL^{OP})_y$] and α-*i*PrO,ω-(C(O)CH=$CHCH_2OP(O)Ph_2$)-[$P(BPL^{Me})_x$-*co*-$(BPL^{OP})_{y-1}$] have the same formulae and cannot be distinguished by MS. Yet, the two populations can be distinguished by NMR, as the crotonate derived from $BPL^{Me}$ has $^1$H signals at δ 5.77 and 1.85 ppm (Figure 1), while the crotonate derived from $BPL^{OP}$ has $^1$H signals at δ 6.20 and 4.85 ppm (Figures S8 and S11). Only the former signals were observed in the recovered polymers (Figure 1), indicating that termination by –(C(O)CH=$CHCH_2OP(O)Ph_2$ is minimal, if any.

[54] We also observed small amounts of the ring-opening product of $BPL^{OP}$ by *i*PrOH, of the corresponding dimer, i.e. α-*i*PrO,ω-OH-[$P(BPL^{OP})_2$], as well as of α-*i*PrO,ω-(C(O)CH=$CHCH_3$)-[$(BPL^{OP})_2$] and/or α-*i*PrO,ω-(C(O)CH=$CHCH_2OP(O)Ph_2$)-[$P(BPL^{Me})_1$-*co*-$(BPL^{OP})_1$] (the latter two products have the same formulae and cannot be distinguished); no higher oligomers ($y > 3$) of $BPL^{OP}$ were detected; see Table S2.

[55] In addition to these three series of $P(BPL^{OP})_x$-*co*-$(BPL^{Me})_y$ macromolecules, another one with α,ω-HO/H terminal groups was also identified (see Figure 5 and Table S2). Its relative intensity varied from one to another sample, and even more depending on the ESI MS analytical conditions. In particular, this population was much exacerbated when ESI MS was conducted in MeOH with 0.1 wt% of formic acid. We assume it arises from acidic hydrolysis of α,ω-*i*PrO/H linear or cyclic chains during final catalytic workup or ESI MS analyses.